Metabolomic and Transcriptomic Analysis of *Lycium chinese* and *L. ruthenicum* Under Salinity Stress

Xiaoya Qin (qinxiaoya@whu.edu.cn)
Wolfberry Engineering Research Institute, Ningxia Academy of Agriculture and Forestry Sciences, National Wolfberry Engineering Research Center

Yue Yin
Wolfberry Engineering Research Institute, Ningxia Academy of Agriculture and Forestry Sciences, National Wolfberry Engineering Research Center

Jianhua Zhao
Wolfberry Engineering Research Institute, Ningxia Academy of Agriculture and Forestry Sciences, National Wolfberry Engineering Research Center

Wei An
Wolfberry Engineering Research Institute, Ningxia Academy of Agriculture and Forestry Sciences, National Wolfberry Engineering Research Center

Yunfang Fan
Wolfberry Engineering Research Institute, Ningxia Academy of Agriculture and Forestry Sciences, National Wolfberry Engineering Research Center

Xiaojie Liang
Wolfberry Engineering Research Institute, Ningxia Academy of Agriculture and Forestry Sciences, National Wolfberry Engineering Research Center

Youlong Cao
Wolfberry Engineering Research Institute, Ningxia Academy of Agriculture and Forestry Sciences, National Wolfberry Engineering Research Center

---

Research Article

Keywords: wolfberry, Lycium. chinese, Lycium. ruthenicum, salinity stress, abscisic acid, flavone, flavonoid

Posted Date: April 8th, 2021

DOI: https://doi.org/10.21203/rs.3.rs-384516/v1

Version of Record: A version of this preprint was published at BMC Plant Biology on January 3rd, 2022.
See the published version at https://doi.org/10.1186/s12870-021-03375-x.

Abstract

Background: High soil salinity often adversely affects plant physiology and agricultural productivity of almost all crops worldwide, including the crude drug known as wolfberry. However, the mechanistic basis of this action in wolfberry is not fully understood yet.

Results: Here in this study, we studied potentials different mechanisms in Chinese wolfberry (*Lycium chinese*, LC*)* and black wolfberry (*L. ruthenicum*, LR*)* under salinity stress, by analyzing their transcriptome and metabolome. The hormone detection analysis revealed that the ABA content was significantly lower in LR than LC under normal conditions, but increased sharply under salinity stress in LR but not in LC. The transcriptome analysis showed that the enriched salinity-responsive genes in wolfberry were mainly related to MAPK signaling, amino sugar and nucleotide sugar metabolism, carbon metabolism, and plant hormone signal transduction pathways in LC, while mainly related to carbon metabolism and protein processing in endoplasmic reticulum in LR. Metabolome results indicated that LR harbored higher flavone and flavonoid content than LC under normal conditions. However, when exposed to salinity stress, flavone and flavonoid content hardly changed in LR, whereas flavonoid and flavone biosynthesis was activated to resist to salinity stress in LC.

Conclusions: Our results adds ABA and flavone metabolism to mechanistic understanding of salinity tolerance in wolfberry. In addition, flavone play a positive role in resistance to salinity stress in wolfberry.

Background

Currently, more than one-third of the world's agricultural acreage is affected by salinization. Soil salinity is a worsening global problem that impairs plant growth and crop yield, posing serious problems to modern agriculture [1]. Accordingly, perhaps the most efficient way to prevent such crop production losses induced by salinity is to cultivate salt-tolerant plant varieties. Hence, a better understanding of the mechanisms by which plants respond to salt stress becomes imperative, as this will help to improve tolerance to salinity in crops via biotechnological approaches. To achieve this goal, it is imperative to study the salt-tolerance mechanisms of plants native to high-salinity environments, such as wolfberry. For example, the leaves of *Lycium ruthenicum* are notably thickened to adapt to high salinity conditions. Importantly, salinity stress can suppress plants' growth and impair their development at multiple scales, such as physiological, phytohormone, and metabolism.

In terms of physiological responses, salinity stress typically induces osmotic stress and ionic imbalance in plants. Osmotic stress accompanied with salinity stress gives rise to the rapid closure of stomata which reduces the plant's ability to absorb CO_2 [2]. Furthermore, the ionic imbalance induced by the excessive accumulation of Na^+ and Cl^- results in ionic toxicity, which does harm to plant and may even kill it by inhibiting the activity of enzymes under salinity stress conditions [3]. Since Na^+ is similar to K^+, any surplus Na^+ would replace K^+ in some enzymatic reactions to reduce various enzyme activities, such as those involved in primary metabolism, glycolysis, and Calvin cycle [4, 5]. Superabundant Cl^- in the

shoot tissue can replace the non-selective anion transporters of NO_3^- and SO_4^{2-}, thereby leading to a shortage of key macro-nutrients like N and S in the affected plants [6].

Furthermore, being a versatile signal, reactive oxygen species (ROS) are rapidly induced by salinity stress, mainly in the apoplast, chloroplast, mitochondria, and peroxisomes [7]. The *AtRbohD* and *AtRbohF* genes responsible for ROS production are both up-regulated under high salinity [8]. Several studies have revealed that *AtRbohD* and *AtRbohF* play positive roles in the salt stress tolerance of plants. ROS production from *AtRbohD* and *AtRbohF* at the early stage of salt stress contributes to lignin formation under saline environment and this reduces oxidative damage to cells [8]. At low concentrations, ROS often act as normal signals in regulating many biological processes, but when in excess they play a harmful effector role in plant growth, which manifests as lipid peroxidation in cellular membrane, protein denaturation, and impairment of enzymatic activities [9]. The greater ion fluxes across the thylakoid membrane via ion channels, as activated by H_2O_2, cause thylakoids to swell, leaving the photosynthetic performance of chloroplasts diminished [10, 11].

Many sensors operate along the salt stress-signaling pathway to transduce signals to the interior of cells and to adjust cellular traits, to avoid damage caused by high salt concentrations. High salinity has been shown to increase the cytosolic Ca^{2+} concentration within just seconds to minutes [12, 13]. Recently, researchers have identified that glycosyl inositol phosphorylceramide (GIPC) sphingolipids directly bind to Na^+ and can regulate the entry of Ca^{2+} into cytosol [14]. Some other proteins also have been reported as mediators in salt-induced Ca^{2+} signaling, namely FERONIA(FER), annexin1 (ANN1) and plastid K^+ exchange antiporters (KEAs) [15–17]. The cell wall-localized leucine-rich repeat extensions LRA3, LRX4, and LRX5 participate in the sensing and relaying of salt stress signals by monitoring the status of cell wall integrity, and function together with secretory peptides RALFs and the receptor-like kinase FER [18].

High salinity also induces osmotic stress in plants as well as organellar stress such as chloroplast stress. For example, the SNF1-related protein kinase 2s (SnRK2) can be activated by osmotic stress in an ABA-dependent or ABA-independent manner, which contributes to greater inhibition of plant growth and promotes leaf chlorosis under osmotic stress [19–21]. Moreover, the biosynthesis of amino acids, fatty acids, and lipids occurs in chloroplasts [22]. The photosynthetic impairments arising from by damaged chloroplast is a major reason why plant growth is inhibited under salt stress [23, 24]. Most ABA biosynthesis-associated proteins, such as ABA1, ABA4, and NCED3, are localized in chloroplast where most of the steps in ABA biosynthesis also take place, which are required in ABA accumulation that induced by salt stress [25]. As the predominant phytohormone involved in the plant response to salinity stress, ABA increases rapidly and massively in root and leaf tissues within just several minutes [26, 27]. Furthermore, it has been reported that precursors transported from leaves are required for ABA synthesis in roots [28]; the stress-induced augmentation of ABA levels in roots is several fold higher than in leaves [27] and salinity stress is known to induce a significant accumulation of ROS in plant roots [29]. In this respect, ABA can interact with H_2O_2 in plant systemic responses to abiotic stresses [30]. For osmotic

stress to induce greater H_2O_2 production requires NADPH oxidase, with the latter was stimulated by ABA [31].

The accumulation of compatible osmolytes helps plants maintain a low intracellular osmotic potential under conditions of high salinity [32, 33], including proline, glycine betaine, sugars, and polyamines, among others [34, 35]. Proline in particular is pivotal for an osmotic adjustment under salt stress; it accumulates through the activation of its biosynthesis pathway and the suppression of its catabolic pathway [36]. Furthermore, proline also acts as a ROS scavenger to attenuate oxidative stress and this assists in stabilizing proteins and membrane structures under high salinity [37–39]. Besides proline, some sugars, namely glucose, fructose, and myo-inositol, can also function as signals in plants response to high salinity [40].

Soil salinity will continue to threaten crop production and food security in the future. Therefore, additional research on the dynamics of transcriptome and metabolism networks of plants as they respond to salinity stress is necessarily. Nevertheless, since the ability of plants to tolerate high salinity varies widely among species, this provides an opportunity to identify genes and metabolites that are pivotal for conferring salinity tolerance to plants.

Wolfberry is a genus of perennial shrub (*Lycium* L.), in the Solanceae family, whose distribution in China ranges across Xinjiang, Ningxia, Qinghai, Gansu, and Neimenggu provinces. The black wolfberry species (*L. ruthenicum*, LR) generally occurs in saline soil or in desert ecosystems, being a typical wild plant that is both drought-resistant and salt-tolerant, which also has high economic and nutritive values in China. Black wolfberry is recognized for its many advantages in cultivation, mainly its resistance to drought and cold, and its tolerance of salinity. Surprisingly, only few studies have investigated the molecular mechanism underpinning black wolfberry's salinity resistance. In this study, its differentially expressed genes and metabolites were analyzed and filtered via transcriptome and metabolism sequencing techniques. Furthermore, complementing this, we also investigated Chinese wolfberry (*L. chinese*, LC) response to salinity stress, with the differences between the stress responses of LC and LR analyzed by examining their transcriptome and metabolome. With these results, the molecular mechanisms of tolerance to salinity stress in black and Chinese wolfberry could be revealed, as well as identifying the key players involved, to improve our understanding of how these species respond to salinity stress.

Results

Phenotypic differences between *L. chinese* and *L. ruthenicum* in response to salinity stress

To investigate the effects of salinity stress on growth and development of wolfberry and the possible mechanism regulating the response to high salinity, Chinese wolfberry (*Lycium. Chinese*) and black wolfberry (*Lycium. Ruthenicum*) were selected as experimental materials. Firstly, the growth state of LC and LR was examined, by planting twig cuttings in the Murashige and Skoog (MS) medium containing 0 mM (control), 150 mM, 200 mM, 250 mM, and 300 mM of NaCl. Figure 1a shows images taken after

three weeks cultivation. The growth of wolfberry seedlings was increasingly inhibited by salinity stress, they had fewer and shorter roots under higher salt concentrations, and their leaf numbers were reduced and more yellowing. For LR, its leaves displayed a sharp yellowing phenomenon and roots were notably shortened under 300 mM NaCl condition; this phenomenon was found in LC as well, but under 200 mM NaCl condition. Hence, the capacity to withstand salinity stress was significantly weaker in LC than LR seedlings.

The seed germination rate of LC and LR under salinity stress was also tested. As Fig. 1b and 1c show, germination rate was more severely impaired in LC than LR; the germination in LR was higher and occurred sooner than LC under the control condition and 150 mM NaCl concentration. Furthermore, relative to the control, more sown seeds of LR (86%) germinated than those of LC (18%), indicating the ability to germinate of LC is severely hindered by salinity stress, but not LR.

Hormone changes in wolfberry in response to salinity stress

To further explore the differences between LC and LR in tolerance to salinity, the abscisic acid (ABA), jasmonic acid (JA), and salicylic acid (SA) content in the leaves of LC and LR under control and 150 mM NaCl conditions were tested. As Fig. 2 shows, for the control group, the ABA content in LR was significantly lower than that in LC. Compared with the control condition, 150 mM NaCl treatment induced the ABA content slightly increase in LC leaves, but this was not a significant difference, whereas a significantly large amount of ABA accumulated in the leaves of LR (Fig. 2a). Further, the JA content was significantly higher in leaves of LR than LC under the control condition, though JA accumulation was significantly reduced by salinity stress, more in LR than in LC (Fig. 2b). The SA content in the leaves of LR was lower than that in LC under control condition, but was not significantly affected by the salinity treatment in both species (Fig. 2c). These results indicated that the tolerance to high salinity stress in LR was driven by accumulating ABA while reducing its JA content.

Overview of the transcriptomic responses of LC and LR to salt stress

To better understand the molecular basis of salinity stress responses in LC and LR, we carried out transcriptome sequencing and analyzed different expressed genes (DEGs) between LC and LR under control or salinity conditions. A total of 2836 DEGS were detected in LC under salinity stress compared with the control group, in which 1337 genes were up-regulated and 1499 genes down-regulated. For LR, however, only 141 genes were differentially expressed when treated with high salinity,in which 80 genes were up-regulated and 61 genes were down-regulated (Fig. 3a). To identify the key determinate factors of the transcriptome, PCA was performed on the genes of the two species under control or salinity treatment conditions. The first two principal components (PC1, PC2) were able completely distinguish our combinations of species and treatment (i.e., 2 species x 2 treatment levels [mock and 150mM salinity concentration]). The PCA shows a clear separation between the wolfberry species along PC1 and the separation of treatment can be observed along PC2. In addition, the three biological replicates were projected closely in the ordination space, which suggested a good correlation between replicates (Fig. 3b). A Venn diagram was used to analyze and display the differences between variation genes of LC

and LR under salinity stress respectively. As depicted in Fig. 3c, group LC-mock vs. LC-NaCl and group LR-mock vs. LR-NaCl only shared two changed genes in total under salinity stress.

KEGG enrichment analysis of DEGs in LC and LR under salinity stress

Evidently, as shown in Fig. 4a, for LC-mock vs. LC-NaCl, the differential genes in LC between the control and salinity condition are mainly enriched in metabolic pathways (48.57%), biosynthesis of secondary metabolites (22.81%), plant–pathogen interaction pathway (10.26%), MAPK signaling pathway (6.16%), amino sugar and nucleotide sugar metabolism pathway (6.16%), carbon metabolism (5.47%), and plant hormone signal transduction (5.02%). For the group LR-mock vs. LR-NaCl (Fig. 4b), the DEGs in LR between control and salinity condition are mainly enriched in metabolic pathways (60%), biosynthesis of secondary metabolites (38.18%), carbon metabolism, protein processing in endoplasmic reticulum, spliceosome, tryptophan metabolism, and lysine degradation..

Dynamic transcriptome analysis between LC and LR in response to salinity stress

To study the genes expression patterns in LC and LR under background and salinity conditions, a K-means cluster analysis was performed, in which the expression patterns of genes of the LC-mock, LC-NaCl, LR-mock, and LR-NaCl groups of wolfberry plants were classified into 10 subclasses; these were then roughly divided into six categories (Fig. 5). The first category was class of genes that showed no regulation change in LC when subjected to salinity stress compared with the background condition, yet they showed a trend of up-regulation in LR (subclass1, subclass9). The second category, by contrast, was a class of genes whose regulation levels also went unchanged under salinity stress (compared with background condition) in LC but whose tendency was to become down-regulated in LR under salinity stress (subclass7, subclass8). The third category of genes featured an up-regulated expression trend under salinity stress in LC, which remained unchanged under salinity stress in LR (subclass2, subclass3). The genes of the fourth category were instead down-regulated in LC under salinity stress while their expression levels were mostly unchanged in LR (subclass6, subclass10). Concerning the fifth category genes, under salinity stress, they were up-regulated in LC yet down-regulated in LR when exposed to high salinity stress(subclass4). The sixth category of genes had expression levels not induced by salinity stress in either LC or LR (subclass5).

KEGG pathway enrichment analysis was carried out for the 10 subclasses. These results demonstrated that these DEGs were mainly involved in metabolic pathways and biosynthesis of secondary metabolites pathways. For the first category, the first five pathways in both subclass1 and subclass9 are plant–pathogen interaction, plant hormone signal transduction, carbon metabolism, MAPK signaling pathway, and RNA transport. For the second category, the first five pathways in subclass7 are protein processing in endoplasmic reticulum, carbon metabolism, starch and sucrose metabolism, plant–pathogen interaction, and phenylpropanoid biosynthesis; the first five pathways in subclass8 are plant–pathogen interaction, ribosome, carbon metabolism, plant hormone signal transduction, and biosynthesis of amino acids. For the third category, the first five pathways in subclass2 and subclass3 are plant–pathogen interaction, plant hormone signal transduction, protein processing in endoplasmic reticulum, MAPK signaling pathway, and carbon metabolism. For the fourth category, the first five pathways in subclass6 and

subclass10 are carbon metabolism, plant hormone signal transduction, biosynthesis of amino acids, starch and sucrose metabolism, and MAPK signaling pathway. For the fifth category, the main enriched pathways in subclass4 are plant–pathogen interaction, and protein processing in endoplasmic reticulum. For the sixth category, the main enriched pathways in subclass5 are plant–pathogen interaction, carbon metabolism, ribosome, biosynthesis of amino acids, and RNA transport.

Metabolomic analysis of LC and LR responses to salinity stress

Next, the metabolites of Chinese wolfberry and black wolfberry plants under salinity stress were detected, and the difference in the metabolites between species or conditions was analyzed. As Fig. 6a shows, for 80 metabolites in LC, their expression levels were changed under salinity stress, in which 57 were up-regulated and 23 were down-regulated. The expression levels of 69 metabolites in LR were changed under salinity stress, in which 34 were up-regulated and 35 were down-regulated. Compared with LC, 207 metabolites were differentially expressed in the leaves of LR under background condition,in which 151 were up-regulated and 56 were down-regulated. In all, 234 metabolites were differentially expressed in the leaves between LC and LR under salinity stress, of which 146 were up-regulated and 88 were down-regulated. The PCA of the metabolites in the control group and the salt treatment group of LC and LR showed that PC1 and PC2 could completely distinguish the four combinations of species and treatment (Fig. 6b). In Fig. 6c, the difference in metabolites' change between different comparative groups is summarized (using a Venn diagram). Groups LC-mock vs. LC-NaCl and LR-mock vs. LR-NaCl shared eight metabolites with common changes,in which seven were up-regulated, and one was down-regulated. Compared with LC-mock vs. LR-mock, the group LC-NaCl vs. LR-NaCl had 161 metabolites featuring the same change tendency, 113 of which were up-regulated and 48 down-regulated. In the other comparisons, LC-mock vs. LR-mock and LC-mock vs. LC-NaCl, 25 metabolites had the same trend in variation, all of which were up-regulated.

KEGG enrichment analysis of different metabolites in LC and LR under salinity stress.

The metabolites in the four comparison groups (LC-mock vs. LC-NaCl, LR-mock vs. LR-NaCl, LC-mock vs. LR-mock, LC-NaCl vs. LR-NaCl) were enriched by KEGG, with the results summarized in Fig. 7. All the metabolites were mainly enriched in metabolic pathways and biosynthesis of secondary metabolites pathways, followed by a detailed analysis of other enrichment pathways. As seen in Fig. 7a, in the group LC-mock vs. LC-NaCl, the changes in metabolites induced by salinity stress in LC mainly concerned these pathways: microbial metabolism in diverse environments, biosynthesis of alkaloids derived from shikimate pathway, biosynthesis of phenylpropanoids, arginine and proline metabolism, and flavone and flavonol biosynthesis. In Fig. 7b, for the group LR-mock vs. LR-NaCl, the metabolites variation induced by salinity stress in the leaves of LR were mainly enriched in the following pathways: biosynthesis of amino acids, purine metabolism, cysteine and methionine metabolism, biosynthesis of amino acids, and protein digestion and absorption. For the group LC-mock vs. LR-mock (Fig. 7c), the different metabolites between leaves of LC and LR at the background condition were mainly concentrated in five pathways: microbial metabolism in diverse environments, pyrimidine metabolism, purine metabolism, flavone and flavonol biosynthesis, and biosynthesis of phenylpropanoids. Finally, in the LC-NaCl vs. LR-NaCl group (Fig. 7d)

the disparity in leaf metabolites between LC and LR under salinity pressure mainly arose in these pathways: microbial metabolism in diverse environments, purine metabolism, tryptophan metabolism, phenylpropanoid biosynthesis, and flavone and flavonol biosynthesis.

Analysis of top 20 differentially expressed metabolites in LC and LR under normal and salinity stress conditions

The top 20 differentially expressed metabolites with more significant log_2FC whose expression pattern matched their related genes in the four comparison groups (LC-mock vs. LC-NaCl, LR-mock vs. LR-NaCl, LC-mock vs. LR-mock, LC-NaCl vs. LR-NaCl) are shown in Fig. 8. In the group LC-mock vs. LC-NaCl, these highly ranked metabolites were linked to flavonol, anthocyanins, polyamine, nucleotide and its derivatives, organic acids and quinate. More specifically, most flavonols, including hyperoside, hyperin, avicularin, and biorobin, were down-regulated in LC when exposed to salinity. In the anthocyanins classification, malvidin-3-O-rutinoside-5-O-glucosides were up-regulated, while both delphinidin 3-galaactoside chloride and procyanidin B2 were down-regulated. The polyamines were up-regulated, while the nucleotide and its derivatives were down-regulated (Fig. 8a). In the group LR-mock vs. LR-NaCl, the primarily changed metabolites were associated with amino acids derivatives, nucleotide and its derivatives, polyamine, vitamins, anthocyanin, coumarins, nicotinic acid derivatives, hydroxycinnamoyl derivatives, and organic acids. Examined in greater detail, the amino acids derivatives, 3-hydroxykynurenine and L-(-)-cystine were all down-regulated, whereas S-(5'-adenosy)-L- homocysteine and L-cysteine were both up-regulated during salinity stress. Nucleotide and its derivatives, such as adenosine 5'-monophosphate, adenine, and iP7G, along with the polyamines, such as N-sinapoyl cadaverine, diCaf-put, and N-sinapoyl putrescine, in addition to the organic acids like D-erythronolactone, were all up-regulated in LR when exposed to high salinity. Furthermore, some vitamins, namely nicotinamide-N-oxide and (-)-riboflavin, were down-regulated in LR during salinity stress (Fig. 8b). In the group LC-mock vs. LR-mock, under background conditions, the main differential metabolites found were flavonoid, anthocyanins, and polyamine. Some flavonoids were up-regulated in LR compared with LC, like C-hexosyl-apigenin O-caffeoylhexoside, C-hexosyl-tricetin O-pentoside and isorhamnetin rutinose, but others were evidently down-regulated, such as hesperetin C-hexosyl-O-hexosyl-O-hexoside, kaempferol-3-O-glucoside-7-O-soph, luteolin O-hexosyl-O-hexoside and quercetin-3-O-glucose-7-O-soph (Fig. 8c). In the group LC-NaCl _vs._ LR-NaCl, the major differential metabolites in LR compared with LC under salinity stress were related to flavonoid anthocyanins and polyamine. Most of the gathered anthocyanins and polyamines were down-regulated in LR compared with LC under high salinity. In the flavonoid classification (Fig. 8d), some were up-regulated in LR compared with LC—e.g., C-hexosyl-tricetin O-pentoside, quercetin-O-glucoside, isoquercitroside, physcion-8-O-β-D-glucoside, biorobin and C-hexosyl-apigenin O-caffeoylhexoside—while several other flavonoids were down-regulated in LR compared with LC under salinity stress (such as kaempferol-3-O-glucoside-7-O-soph, luteolin O-hexosyl-O-hexosyl-O-hexoside, and quercetin-3-O-glucose-7-O-soph).

KEGG pathway enrichment in DEGs and different metabolites in LC and LR

According to the above KEGG enrichment analysis, a histogram was drawn to show the common pathways in which DEGs and differential expressed metabolites were highly enriched in. As Fig. 9 shows, in which a taller ordinate column corresponds to greater enrichment. In group LC-mock vs. LC-NaCl (Fig. 9a), the metabolic pathways distinguished by a simultaneously higher enrichment of DEGs and differential metabolites are arginine and protein metabolism, benzoxazinoid biosynthesis, and riboflavin metabolism. In group LR-mock vs. LR-NaCl (Fig. 9b), the corresponding metabolic pathways are lysine degradation pathway, nitrogen metabolism, and purine metabolism.

Flavonoid metabolism in LC and LR during salinity stress

Flavonoid metabolism plays an important role in protecting plants against adverse effects of salinity stress. Figure 10a illustrates the flavonoid biosynthesis pathway, for which the marked genes that were analyzed appear in Fig. 10b. The expression profiles of almost all these marked genes in the flavonoid metabolism pathway had a pattern of lower abundance in LR than LC, either under the background condition or salinity stress. Specifically, the genes encoding chalcone synthase (Cluster-40571.102907), flavone synthase II, 2-hydroxyisoflavanone synthase-like (Cluster-40571.125750), and flavonol synthase, and flavonol synthase/flavanone 3-hydroxylase (Cluster-40571.25710) were apparently not in LR but up-regulated in LC when wolfberry plants were exposed to salinity stress. However, the genes for flavone synthase II, 2-hydroxyisoflavanone synthase-like (Cluster-40571.123809), flavone synthase II, 2-hydroxyisoflavanone synthase-like (Cluster-40571.199168), and flavonoid 3’-monooxygenase, flavonoid 3’-monooxygenase (Cluster-40571.294286) were all no-regulated in LR yet down-regulated in LC during salinity stress. Moreover, the genes encoding naringenin 3-dioxygenase and naringenin 2-oxoglutarate 3-dioxygenase (Cluster-40571.120883) were up-regulated in both LC and LR under salinity stress, while that for naringenin 3-dioxygenase (Cluster-40571.135119) was up-regulated in LR but non-regulated in LC. Furthermore, the genes for flavone synthase II, 2-hydroxyisoflavanone synthase-like (Cluster-40571.303908) were down-regulated both in LR and LC in salinity stress conditions (Fig. 10b). Interestingly, most of the changed metabolites in the flavonoid biosynthesis pathway during salinity stress persisted in higher abundance in LR but at a lower level in LC. Including butin, catechin, neohesperidin, naringenin, and afzelecin; in which, butin was down-regulated both in LR and LC, catechin was non-regulated in LR but up-regulated in LC, neohesperidin was up-regulated in LR but down-regulated in LC, naringenin was down-regulated in LR but up-regulated in LC, and afzelechin was non-regulated in LR but up-regulated in LC. Apart from those metabolites, eriodictyol remained at a lower level in LR than LC, yet it was down-regulated in LR though not regulated in LC. While pinocembrin also occurred at a low level in LR than LC, it was up-regulated in both LR and LC. In contrast, chlorogenic acid was generally higher LR than LC, and it was up-regulated in LR but down-regulated in LC (Fig. 10c).'

Alterations in flavone and flavonol metabolism in LC and LR after exposure to high salinity

It is noteworthy that the flavone and flavonol biosynthesis pathway was enriched significantly in both transcriptomic and metabolomic data of wolfberry plants. The flavone and flavonol biosynthesis pathway appears in Fig. 11a, and the marked expression pattern of relative genes are detailed in Fig. 11b. This revealed that most of the genes involved in flavone and flavonol biosynthesis pathway stay constitutively expressed at low level in LR but at a higher level in LC, such as flavonol-3-O-glucoside

glucosyltransferase (Cluster-40571.113183) and galactoside glucosyltransferase (Cluster-40571.291876), although both their expression levels went unchanged during salinity stress in both species. For glucosyltransferase (Cluster-40571.113184), flavonol-3-O-glucoside galactoside glucosyltransferase (Cluster-40571.249135), and flavonoid 3’-monooxygenase (Cluster-40571.294286), their transcription levels were high in LC and low in LR, and down-regulated in LC but not-regulated in LR, when exposed to salinity stress. Regarding flavonol-3-O-glucoside L-rhamnosyltransferase (Cluster-40571.163208) and kaempferol 3-O-beta-D-galactosyltransferase (Cluster-40571. 188476), their abundance of transcripts were higher in LC than LR, with expression up-regulated in LC yet non-regulated in LR during salinity stress. Besides, some other genes—including the novel plant SNARE (Cluster-40571.242780), flavonoid 3’-monooxygenase (Cluster-40571.294284), and flavonoid 3’-monooxygenase-like (Cluster-40571.294288), showed consistently greater expression in LR than LC, with transcription levels up-regulated in LR but down-regulated or not regulated in LC when the plants were exposed to salinity stress (Fig. 11b). Further, for most of the changed metabolites in flavone and flavonol biosynthesis pathway during salinity stress in wolfberry, their content stayed at a high level in LR but a lower level in LC. As seen in Fig. 11c, the 3,7-di-O-methylquercetin continued to have a lower content under the background condition, but this was up-regulated to greater extent in LC and down-regulated in LR when the plants were exposed to salinity stress. Moreover, isovitexin, astragalin, and cosmosiin had contents that stayed at higher level in LR than LC under the background condition, yet under salinity stress both of them were down-regulated in LR and LC. The rutin content was found to be higher in LR than LC, but this did not change during salinity stress. This was not so for cynaroside, whose background content remained low in LC but high in LR, while it was down-regulated in LC and up-regulated in LR under high salinity conditions (Fig. 11c).

Discussion

Soil salinity will continue to threaten crop production and security in the future. Cultivation of salt-tolerant crops is therefore the most effective way to overcome this pressing environmental problem. In this study, we found that black wolfberry was better able to tolerate salinity than Chinese wolfberry.

ABA content is normally low but rises sharply in LR plants exposed to high salinity

ABA is involved in the growth and development regulation of plants, such as inhibiting seed germination, promoting dormancy, causing stomatal closure, inhibiting growth, and promoting leaf senescence and shedding [41]. At the same time, it also plays a vital role in coping with a variety of stresses that plants might incur in nature [42]. ABA is a hormone with a low content yet great effect in plants. Under stressful conditions, the ABA concentration will increase and induce changes in certain metabolic processes in plants and in this way will play a role in resistance to adversity. Salinity stress leads to much ABA accumulating in plant roots, which is transported to the aboveground parts via xylem fluid flow. As a result, ABA accumulation in leaves delays the leaf expansion rate and promotes stomatal closure, which reduces the transpiration rate of plants and the transport of salt in root caps, thus alleviating the damage to plants caused by salinity stress [43].

Comparing LC and LR wolfberry plants, we found that the ABA content in LR was significantly lower than that in LC under normal (non-stressed) growing condition. When exposed to the high salinity condition, the LR quickly accumulated a large amount of ABA to resist salinity stress, but only a small amount of ABA was increased in LC to withstand injury form high salinity. These results confirm the strong resistance to salinity stress of black wolfberry.

Flavone and flavonoid stay at a higher content statement under non-stressed condition than salinity stress in LR

Flavonoids constitute a class of important secondary metabolites widely found in plants, and they can affect many traits of plants (e.g. edibleness, stress resistance, to name a few) [44]. Flavonoids play a key role in plant growth and protection against extreme environments [45, 46]. The type, content, distribution, and function of particular flavonoids vary greatly among species but also differ among plant tissues and even across development stages. During the growth and development of a plant, the metabolites of flavonoids are in a process of dynamic change [47–49]. Many studies have reported that the metabolism of flavonoids is involved in and figures prominently in how plants respond to biotic and abiotic stressors, such as salinity stress, oxidative stress, drought stress, insect chewing, and others [50–52]. Flavonoids can improve the adaptability of plants to adversity by eliminating the accumulation of ROS, or by cooperating with other stress response factors (such as ABA and GA) to mitigate the damage caused by adverse biotic or abiotic factors [53–55].

In this paper, through the joint analysis of wolfberry plants transcriptome and metabolome, we find that irrespective of exposure to salinity stress (i.e., with or without), flavonoids and flavonoids in LR occurred at significantly higher content than in LC, which likely promoted the high salinity tolerance of LR. In addition, by comparing their content in leaves under salinity stress and normal growing conditions, it was found that the accumulation of flavonoids and flavonoids was significantly augmented under high salinity stress in LC, indicating this species needed more flavones to resist the harm caused from high salt stress. However, high salinity stress did not likewise induce a large accumulation of flavonoids in LR, perhaps because the already higher content of flavonoids in this plant under normal conditions was sufficient to resist high salinity stress. This would also explain the higher tolerance of black wolfberry to salinity stress.

Conclusions

To sum up, through this study, we have shown that LR possesses a lower ABA content and a higher level of flavonoids under ambient (background) conditions to resist high salinity stress. Furthermore, when exposed to a high salinity environment, these LR plants will improve their resistance by accumulating much ABA on one hand, while on the other hand mitigating oxidative stress caused by high salinity via their high level of flavonoids already present in their tissues. This research not only reveals the intrinsic reason tolerance to high salinity of the black wolfberry, but it also suggests the enhancement of salinity

tolerance in Chinese wolfberry by improving its flavonoids level, through *in vivo* or *in vitro techniques*, which would also simultaneously increase the nutritional value of its fruits and leaves.

Methods

Plant materials and growth conditions

Seedlings of LC and LR used in the experiments were cultured from seeds or tissues. All the wolfberry seeds were surface-sterilized with 25% sodium hypochlorite, and then air-dried inside a horizontal laminar-flow hood, before sowing them on Murashige and Skoog(MS) medium that contained 1% sucrose and 0.8% agar. After stratification at 4°C in the dark for 3 days, the seed plates were transferred into a 10h-light/14h-dark photoperiod growth chamber whose temperature was controlled at 25°C. In addition, the wolfberry twigs were sterilized successively by 0.1% mercuric chloride, 70% ethyl alcohol, sterile water, and dried inside a horizontal laminar-flow hood subsequently. Then cut into the MS medium, and finally moved into the growth chamber to continue growing.

Phenotype characterization

The salinity tolerance of each wolfberry species (LC and LR) was determined experimentally. Firstly, to assess this phenotypic trait at germination stage, sterilized seeds of the two species were germinated on MS medium containing 150 mM of NaCl or control. The germination rate of *LC* and *LR* seeds were recorded after their stratification and development in the growth chamber for a few days. To evaluate salt tolerance at the vegetative growth stage, tissue-cultured seedlings of both wolfberry were cut and inserting into MS medium containing 150 mM NaCl or control, followed by their transferal to the growth chamber to grow continuously.

RNA extractions

Total RNA was extracted from detached leaves with the Trizol reagent (Invitrogen) according to the manufacturer's protocol. The extracted total RNA was treated with RNase-free DNase I (Thermo Scientific) to remove any trace amounts of DNA contamination. Next, the quality and quantity of extracted RNA were determined by measuring the absorbance at A260/A280 and A260/A230 in a spectrophotometer (NanoPhotometer). RNA integrity and its absence of DNA contamination were further verified by agarose gel electrophoresis. The concentration of RNA in a given sample was measured with high accuracy by a fluorimeter (Qubit 2.0), and the integrality of RNA was precisely confirmed by a bioanalyzer (Agilent 2100).

cDNA library construction and sequencing

The mRNA was acquired in two ways: firstly, the mRNA with a polyA tail were enriched by the Oligo(dT) magnetic beads, and secondly, mRNA was obtained by removing rRNA from total RNA. Afterwards, RNA strands were broken into short fragments in a fragmentation buffer. These short-RNA fragments served as a template to synthesize the first strand cDNA with random hexamers. The second strand cDNA was synthesized by dNTPs (dUTP, dATP, dGTP, dCTP), DNA polymerase I, and first strand cDNA immersed together in a buffer solution. The ensuing double-stranded cDNA was purified by AMPure XP beads, after

which the tail of purified double-strand cDNA was repaired, a polyA tail added, and the sequencing joint connected. Patterns were then picked by AMPure XP beads, and the final cDNA library acquired via PCR enrichment. Next, the final cDNA library was determined, mainly quantified by Qubit 2.0 and its insert size detected by an Agilent 2100; the effective concentration was measured accurately by qPCR. After the cDNA library was determined to be qualified, sequencing was carried out using Illumina Hi-Seq.

Transcript splicing

Clean reads were gained after sequencing, filtration, error rate checking, and GC content-distribution checking. These clean reads were assembled to derive the reference sequence used later, by using Trinity software. The transcriptomes were hierarchically clustered by Corset (https://code.google.com/p/corset-project/), a software tool designed for obtaining gene-level counts from any *de novo* transcriptome assembly, from which the longest cluster sequence was designated the unigene for later analysis. This work was performed in the Metware company.

Gene annotations

Using BLAST software, each unigene was compared with several public databases: KEGG (Kyoto Encyclopedia of Genes and Genomes), NR (NCBI non-redundant protein sequences), Swiss-Prot (manually annotated and reviewed protein sequences), GO (Gene Ontology), and KOG/COG (Clusters of Orthologous Groups of proteins). The amino acid sequence of a given unigene was predicted, followed by blasting it against the Pfam (Protein family) database using HMMER software.

Differentially expressed genes (DEGs)

To explore the profiles of DEGs between LR and LC under different salinity conditions, we analyzed gene expression patterns via DESeq2, to obtain robust DEGs sets. The identification of statistically significant DEGS and their respective fold-changes in gene expression level were implemented by an R package. After doing this, the multiple hypothesis testing was performed by first correcting the P-value of each gene to control the False Discovery Rate (FDR), using the Benjamini-Hochberg procedure. The criteria used a for identifying DEGs were a $|\log_2 \text{fold change}| \geq 1$ with an $\text{FDR} < 0.05$.

Functional annotation of DEGs

A cluster analysis of gene expression patterns was done to predict the genes functions and determine their distribution frequency across functional categories. This analysis relied on annotating genes to KEGG database to identify significantly enriched metabolic pathways or signal transduction pathways in DEGs versus the whole-genome background. Gene Ontology (GO) is another way to analyze gene sets, by describing the functioning of DEGs in terms of molecular function, biological progress and cellular component.

Metabolomics

The detached leaves of wolfberry plants (LC and LR) were freeze-dried and ground in a mixer mill. A 100-mg powder subsample was extracted in 1.2 ml of 70% aqueous methanol at 4°C overnight, followed by centrifuging at 10 000 *g* for 10 min; the ensuing supernatant was absorbed and passed through 0.22-μm

pore size filter before its UPLC-MS (Ultra Performance Liquid Chromatography - Tandem Mass Spectrometry) analysis. Then, each extract sample was analyzed in an UPLA-ESI-MS/MS system (UPLC, Shim-pack UFLC SHIMADZU CBM30A system, www.shimadzu.com.cn/;MS, Applied Biosystems. 6500 Q TRAP, www.appliedbiosystems.com.cn/). This work was performed in the Metware company.

Screening of differential metabolites

Differential metabolites should be excavated accurately from multiple perspectives, by applying both univariate and multivariate statistical analyses. The differential metabolites in the wolfberry species (LC and LR) under salinity conditions could be screened out, in a preliminary way, by the variable importance in projection (VIP) value based on the OPLS-DA (Orthogonal Partial Least Squares - Discriminant Analysis) results.The threshold values used for screening would assign a significant difference when the fold change ≥ 2 or ≤ 0.5, in addition to having a VIP ≥ 1.

Enrichment analysis and functional annotation of differential metabolites

The differential metabolites were annotated using the KEGG database and enriched by KEGG pathway, according to the results from the preceding differential metabolites' analysis. The rich factor is a ratio of the number of differential metabolites in corresponding pathway to the total number of metabolites detected and annotated in that pathway. Accordingly, the enrichment degree is inferred to be higher when this ratio has a larger value, In addition, the closer its P-value was to zero, the more outstanding was a given enrichment.

Statistical analysis

All experiments were carried out at least three times, independently, with similar results. All values are presented as means ± SD. Statistical significance was based on unpaired two-sample Student's *t*-tests, as determined in Sigmaplot 10 software. Principal component analysis (PCA) was also performed on all data sets.

Abbreviations

LC, *Lycium. Chinese*; LR, *Lycium. Ruthenicum*; ABA, abscisic acid; H_2O_2, hydrogen peroxide; JA, jasmonic acid; ROS, reactive oxygen species; SA, salicylic acid; MS, Murashige and Skoog; VIP, variable importance in prejection; MDA, Malondialdehyde; TBA, thiobarbituric acid; TCA, trichloroacetic acid; DEGs, differentially expressed genes; PCA: principal component analysis; KEGG, Kyoto Encyclopedia of Genes and Genomes.

Declarations

Acknowledgements

We thank Metware company for transcriptome and metabolome detection.

Authors' contributions

C-YL conceived the research. Q-XY, YY, Z-JH, AW, L-XJ, and F-YF conducted experiments. Q-XY and C-YL analyzed data and wrote the manuscript with the support of YY, Z-JH, AW, L-XJ, and F-YF. All authors read and approved the manuscript.

Funding

This work was supported by the National Natural Science Foundation of China (Grant # 31960536), and the Key Research and Development Project foundation of Ningxia province of China (Grant # 2018BEB04011). The funding organizations paid the experimental fees and publication fees for this research, but did not play any role in the design of the study nor in the collection analysis and interpretation of data, nor in the writing of the manuscript.

Availability of data and materials

The datasets generated and analysed during the current study are available in the supplementary information files. The link address of transcriptome data is https://dataview.ncbi.nlm.nih.gov/object/PRJNA666311?reviewer=ko1g8cgo4piqpi2d4fje9oaf79.

Ethics approval and consent to participate

Plant materials used in this study were from National Wolfberry Engineering Research Center (Yinchuan, China). The laboratory experiments were conducted under logical legislation and permissions.

Consent for publication

Not applicable.

Author details

Wolfberry Engineering Research Institute, Ningxia Academy of Agriculture and Forestry Sciences / National Wolfberry Engineering Research Center, Yinchuan 750002, China.

Competing interests

The authors declare that they have no competing interests.

References

1. FAO (2011) The state of the world's land and water resources for food and agriculture (SOLAW)—managing systems at risk. Food and Agriculture Organization of the United Nations. Rome and Earthscan, London. http://www.fao.org/ag/agl/agll/spush.
2. Wegner, L.H., Stefano, G., Shabala, L., Rossi, M., Mancuso, S., and Shabala, S. (2011). Sequential depolarization of root cortical and stelar cells induced by an acute salt shock implications for Na^+ and K^+ transport into xylem vessels. Plant Cell Environ. 34, 859–869.

3. Cheeseman, J.M. (2013). The integration of activity in saline environments: problems and perspectives. Funct. Plant Biol. 40, 759–774.
4. Benito, B., Haro, R., Amtmann, A., Cuin, T.A., and Dreyer, I. (2014). The twins K^+ and Na^+ in plants. J. Plant Physiol. 171, 723–731.
5. Wu, H.H., Zhang, X.C., Giraldo, J.P., and Shabala, S. (2018). It is not all about sodium: revealing tissue specificity and signalling roles of potassium in plant responses to salt stress. Plant Soil 431, 1–17.
6. Bazihizina, N., Colmer, T.D., Cuin, T.A., Mancuso, S., and Shabala, S. (2019). Friend or foe? Chloride patterning in halophytes. Trends Plant Sci. 24, 142–151.
7. Miller, G., Suzuki, N., Ciftci-Yilmaz, S., and Mittler, R. (2010). Reactive 1645 oxygen species homeostasis and signalling during drought and salinity stresses. Plant, Cell Environ. 33, 453–467.
8. Ma, L., Zhang, H., Sun, L., Jiao, Y., Zhang, G., Miao, C., and Hao, F. (2012). NADPH oxidase AtrbohD and AtrbohF function in ROS-dependent regulation of Na^+/1614 K^+ homeostasis in Arabidopsis under salt stress. J. Exp. Bot. 63, 305–317.
9. Noctor, G., and Foyer, C.H. (1998). Ascorbate and glutathione: keeping active oxygen under control. Annu. Rev. Plant Physiol. Plant Mol. Biol. 49, 249–279.
10. Barhoumi, Z., Djebali, W., Chaïbi, W., Abdelly, C., and Smaoui, A. (2007). Salt impact on photosynthesis and leaf ultrastructure of Aeluropus littoralis. J. Plant Res. 120, 529–537.
11. Pottosin, I., and Shabala, S. (2016). Transport across chloroplast membranes: optimizing photosynthesis for adverse environmental conditions. Mol. Plant 9, 356–370.
12. Dodd, A.N., Kudla, J., and Sanders, D. (2010). The language of calcium signaling. Annu. Rev. Plant Biol. 61, 593–620.
13. Knight, H., Trewavas, A.J., and Knight, M.R. (1997). Calcium signalling in Arabidopsis thaliana responding to drought and salinity. Plant J. 12, 1067–1078.
14. Jiang, Z., Zhou, X., Tao, M., Yuan, F., Liu, L., Wu, F., Wu, X., Xiang, Y., Niu, Y., Liu, F., et al. (2019). Plant cell-surface GIPC sphingolipids sense salt to trigger Ca^{2+} Nature 572, 341-346.
15. Laohavisit, A., Richards, S.L., Shabala, L., Chen, C., Colaço, R.D.D.R., Swarbreck, S.M., Shaw, E., Dark, A., Shabala, S., Shang, Z., et al. (2013). Salinity-induced calcium signaling and root adaptation in Arabidopsis require the calcium regulatory protein annexin1. Plant Physiol. 163, 253–262.
16. Stephan, A.B., Kunz, H.H., Yang, E., and Schroeder, J.I. (2016). Rapid hyperosmotic-induced Ca^{2+} responses in Arabidopsis thaliana exhibit sensory potentiation and involvement of plastidial KEA transporters. Proc. Natl. Acad. Sci. U. S. A. 113, E5242–E5249.
17. Feng, W., Kita, D., Peaucelle, A., Cartwright, H.N., Doan, V., Duan, Q., Liu, M.-C., Maman, J., Steinhorst, L., Schmitz-Thom, I., et al. (2018). The FERONIA receptor kinase maintains cell wall integrity during salt stress through Ca^{2+} Curr. Biol. 28: 666-675.
18. Zhao, C., Zayed, O., Yu, Z., Jiang, W., Zhu, P., Hsu, C.-C., Zhang, L., Tao, W.A., Lozano-Durán, R., and Zhu, J.-K. (2018). Leucine-rich repeat extensin proteins regulate plant salt tolerance in Arabidopsis. Proc. Natl. Acad. Sci. U. S. A. 115, 13123-13128.

19. Boudsocq, M., Barbier-Brygoo, H., and Laurière, C. (2004). Identification of nine sucrose nonfermenting 1-related protein kinases 2 activated by hyperosmotic and saline stresses in Arabidopsis thaliana. J. Biol. Chem. 279, 41758–41766.
20. Fujii, H., Verslues, P.E., and Zhu, J.-K. (2011). Arabidopsis decuple mutant reveals the importance of SnRK2 kinases in osmotic stress responses in vivo. Proc. Natl. Acad. Sci. U. S. A. 108, 1717–1722.
21. McLoughlin, F., Galvan-Ampudia, C.S., Julkowska, M.M., Caarls, L., Van Der Does, D., Laurière, C., Munnik, T., Haring, M.A., and Testerink, C. (2012). The Snf1-related protein kinases SnRK2.4 and SnRK2.10 are involved in maintenance of root system architecture during salt stress. Plant J. 72, 436–449.
22. Chan, K.X., Phua, S.Y., Crisp, P., McQuinn, R., and Pogson, B.J. (2016). Learning the languages of the chloroplast: Retrograde signaling and beyond. Annu. Rev. Plant Biol. 67, 25–53.
23. Chaves, M.M., Flexas, J., and Pinheiro, C. (2009). Photosynthesis under drought and salt stress: regulation mechanisms from whole plant to cell. Ann. Bot. 103, 551–560.
24. Bose, J., Munns, R., Shabala, S., Gilliham, M., Pogson, B., and Tyerman, S.D. (2017). Chloroplast function and ion regulation in plants growing on saline soils: Lessons from halophytes. J. Exp. Bot. 68, 3129–3143.
25. Xiong, L., Lee, H., Ishitani, M., and Zhu, J.K. (2002). Regulation of osmotic stress-responsive gene expression by the LOS6/ABA1 locus in Arabidopsis. J. Biol. Chem. 277, 8588–8596.
26. Jia, W. (2002). Salt-stress-induced ABA accumulation is more sensitively triggered in roots than in shoots. J. Exp. Bot. 53, 2201–2206.
27. Fricke, W., Akhiyarova, G., Veselov, D., and Kudoyarova, G. (2004). Rapid and tissue-specific changes in ABA and in growth rate in response to salinity in barley leaves. J. Exp. Bot. 55, 1115–1123.
28. Zhang, F.P., Sussmilch, F., Nichols, D.S., Cardoso, A.A., Brodribb, T.J., and McAdam, S.A.M. (2018). Leaves, not roots or floral tissue, are the main site of rapid, external pressure-induced ABA biosynthesis in angiosperms. J. Exp. Bot. 69, 1261–1267.
29. Nath, M., Bhatt, D., Jain, A., Saxena, S.C., Saifi, S.K., Yadav, S., Negi, M., Prasad, R., and Tuteja, N. (2019). Salt stress triggers augmented levels of Na^+, Ca^{2+} and ROS and alter stress responsive gene expression in roots of CBL9 and CIPK23 knockout mutants of Arabidopsis thaliana. Environ. Exp. Bot. 161, 265–276.
30. Mittler, R., and Blumwald, E. (2015). The roles of ROS and ABA in systemic acquired acclimation. Plant Cell 27, 64–70.
31. Zhang, Y., Tan, J., Guo, Z., Lu, S., He, S., Shu, W., and Zhou, B. (2009). Increased abscisic acid levels in transgenic tobacco over-expressing 9 cis-epoxycarotenoid dioxygenase influence H_2O_2 and NO production and antioxidant defences. Plant Cell Environ. 32, 509–519.
32. Apse, M.P., and Blumwald, E. (2002). Engineering salt tolerance in plants. Curr. Opin. Biotechnol. 13, 146–150.
33. Munns, R. (2002). Comparative physiology of salt and water stress. Plant, Cell Environ. 25, 239–250.

34. Verslues, P.E., Agarwal, M., Katiyar-Agarwal, S., Zhu, J., and Zhu, J.K. (2006). Methods and concepts in quantifying resistance to drought, salt and freezing, abiotic stresses that affect plant water status. Plant J. 45, 523–539.
35. Henry, C., Bledsoe, S.W., Griffiths, C.A., Kollman, A., Paul, M.J., Sakr, S., and Lagrimini, L.M. (2015). Differential role for trehalose metabolism in salt-stressed maize. Plant Physiol. 169, 1072–1089.
36. Mansour, M.M.F., and Ali, E.F. (2017). Evaluation of proline functions in saline conditions. Phytochemistry 140, 52–68.
37. Ashraf, M., and Foolad, M.R. (2007). Roles of glycine betaine and proline in improving plant abiotic stress resistance. Environ. Exp. Bot. 59, 206–216.
38. Verbruggen, N., and Hermans, C. (2008). Proline accumulation in plants: a review. Amino Acids 35, 753–759.
39. Ben Rejeb, K., Abdelly, C., and Savouré, A. (2014). How reactive oxygen species and proline face stress together. Plant Physiol. Biochem. 80, 278–284.
40. Jayakannan, M., Bose, J., Babourina, O., Rengel, Z., and Shabala, S. (2013). Salicylic acid improves salinity tolerance in Arabidopsis by restoring membrane potential and preventing salt induced K^+ loss via a GORK channel. J. Exp. Bot. 64, 2255–2268.
41. Wasilewska A, Vlad F, Sirichandra C, et al. An update on abscisic acid signaling in plants and more [J]. Molecular Plant, 2008, 1(2):198-217.
42. Dar N A, Amin I, Wani W, et al. Abscisic acid: Akey regulator of abiotic stress tolerance in plants [J]. Plant Gene, 2017, 11: 106-111.
43. Hartung W, Schraut D, Jiang F. Physiology of abscisic acid (ABA) in roots under stress–a review of the relationship between root ABA and radial water and ABA flows [J]. Australian Journal of Agricultural Research, 2005, 56(11):1253-1259.
44. Seymour GB, Chapman NH, Chew BL, Rose JK. Regulation of ripening and opportunities for control in tomato and other fruits. Plant Biotechnology Journal, 2013, 11:269-278.
45. Dicko MH, Gruppen H, Barro C. Impact of phenolic compounds and related enzymes in Sorghum varieties for resistance and susceptibility to biotic and abiotic stresses. Journal of Chemical Ecology, 2005,31:2671-2688.
46. Petrussa E, Braidot E, Zancani M, Peresson C, Bertolini A, Patui S, Vianello A. Flavonoids-biosynthesis, transport and involvement in stress responses. International Journal of Molecular Sciences, 2013, 14:14950-14973.
47. Zu Y, Chen H, Wang W, Jia J, Zhu L, Zhang N. Sugar, phytohormone, tannins and flavonoids changes during the growth and development of *Eupatorium adenophorum*. Bulletin of Botanical Research, 2006, 26:349-355.
48. Makoi J, Ndakidemi P. Changes in plant growth, nutrient dynamics and accumulation of flavonoids and anthocyanins by manipulating the cropping systems involving legumes and cereals. Australian Journal of Agricultural Engineering, 2011, 2:56-65.

49. Choi SH, Ahn JB, Kim HJ, Im NK, Kozukue N, Levin CE, Friedman M. Changes in free amino acid, protein, and flavonoid content in jujube(Ziziphus jujube) fruit during eight stages of growth and antioxidative and cancer cell inhibitory effects by extracts. Journal of Agricultural & Food Chemistry, 2012, 60:10245-10255.
50. Mahajan M, Yadav SK. Overexpression of a tea flavanone 3-hydroxylase gene confers tolerance to salt stress and alternaria solani, in transgenic tobacco. Plant Molecular Biology, 2014, 85:551-573.
51. Luo P, Shen Y, Jin S, Huang S, Cheng X, Wang Z, Li P,Zhao J, Bao M, Ning G. Overexpression of *Rosa rugosa* anthocyanidin reductase enhances tobacco tolerance to abiotic stress through increased ROS scavenging and modulation of ABA signaling. Plant Science, 2016,245:35-49.
52. Zhu LJ, Deng XG,Zou LJ, Zhang DW, Lin HH. Enhancement of stress tolerance in cucumber seedlings by proanthocyanidins. Biologia Plantarum, 2017, 61:323-332.
53. Steyn WJ, Wand SJE, Holcroft DM, Jacobs G. Anthocyanins in vegetative tissues: a proposed unified function in photoprotection. New Phytologist, 2002,155:349-361.
54. Li S, Wang W, Gao J, Yin K, Wang R, Wang C, Petersen M, Mundy J, Qiu J. MYB75 phosphorylation by MPK4 is required for light-induced anthocyanin accumulation in Arabidopsis. Plant Cell, 2016, 28:2866.
55. Zhao, C., Zhang, H., Song, C., Zhu, J.-K., Shabala, S., Mechanisms of plant responses and adaptation to soil salinity, The Innovation (2020), doi: https://doi.org/10.1016/xinn.2020.100017.

Figures

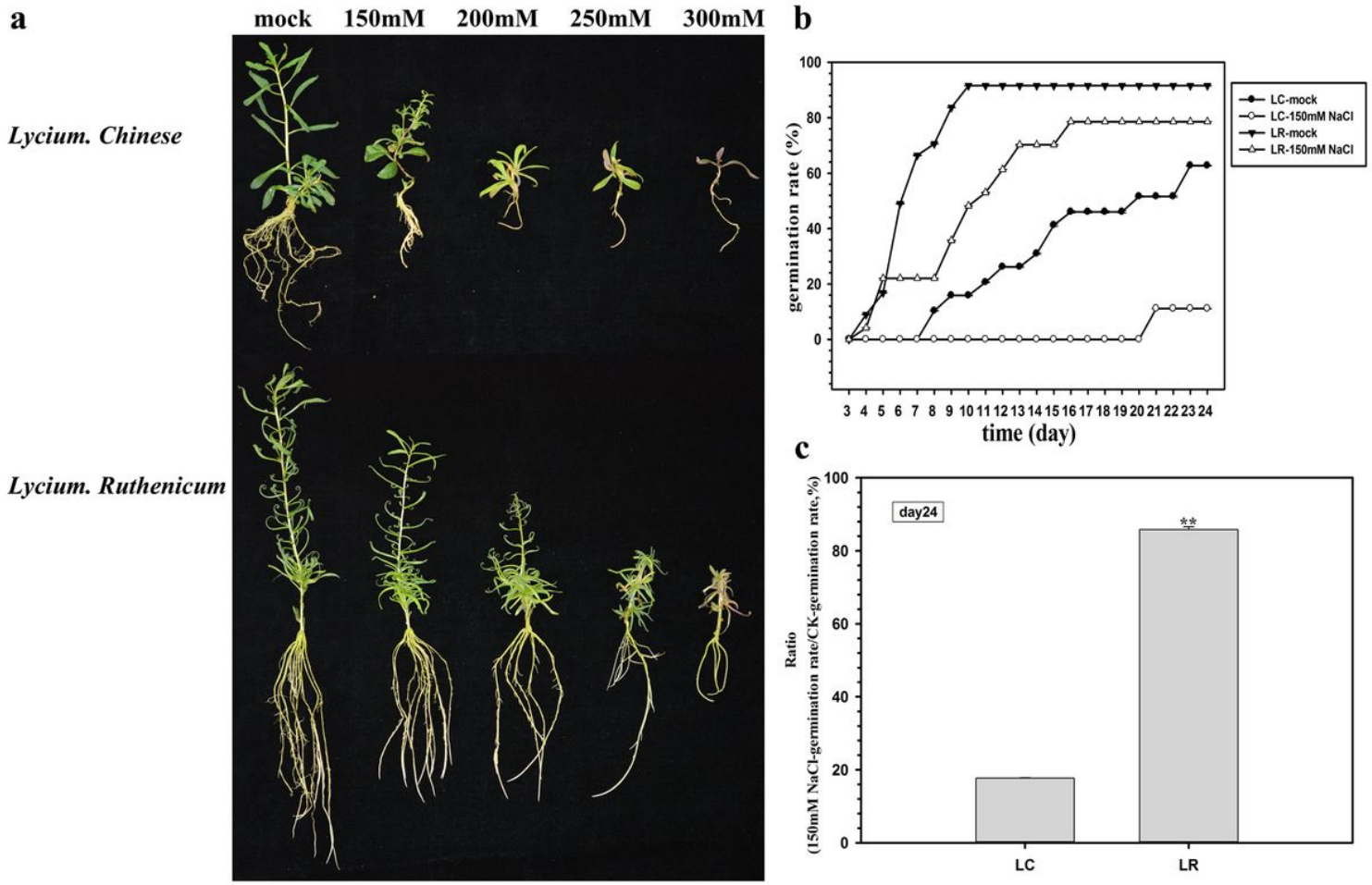

Figure 1

Phenotype analysis of Lycium chinese and L. ruthenicum under salinity stress. a The twig cuttings of L. chinese and L. ruthenicum were planted in the MS medium containing 0 mM (CK), 150 mM, 200 mM, 250 mM or 300 mM of NaCl. Pictures were taken after three weeks of cultivation. b Seed germination rate of L. chinese and L. ruthenicum under control and 150 mM NaCl concentrations was calculated from day 3 to day 24. c The ratio of germination rate 150 mM NaCl/ CK was calculated at day 24 after seeds were sown. * $P < 0.05$, ** $P < 0.01$. N = 3. Bars = means ± SEM.

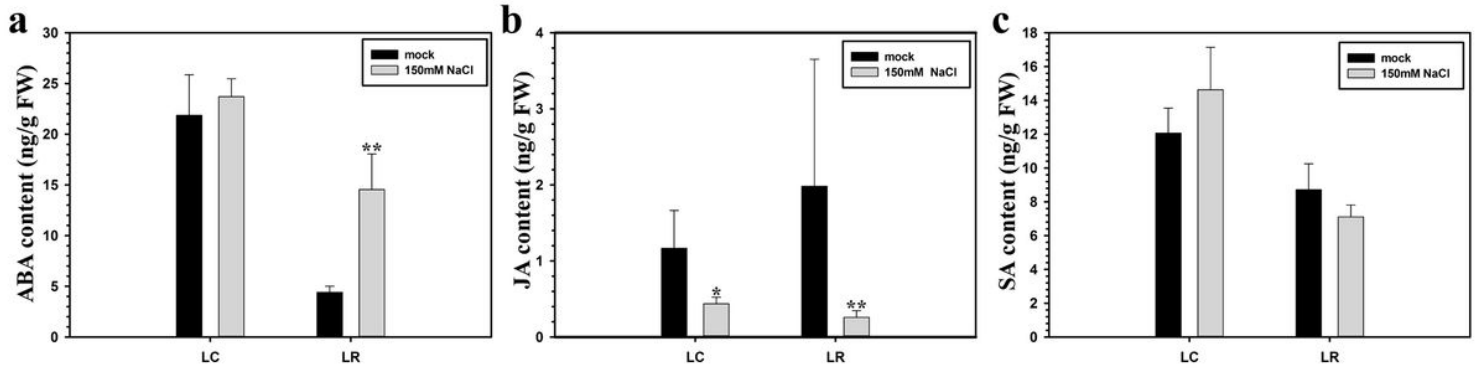

Figure 2

Hormonal variation of Lycium chinese and L. ruthenicum in response to salinity stress. Quantification of ABA (Abscisic acid), JA (Jasmonic acid), and SA (Salicylic acid) contents of L. chinese and L. ruthenicum leaves at indicated time points after NaCl treatment. ABA content in a, JA content in b, and SA content in c. Data represent the means ± SEM of three replicates. Asterisks indicate a significant difference from mock (non-stressed treatment at the same time point (N = 3, Student's t-test: * P < 0.05, ** P < 0.01).

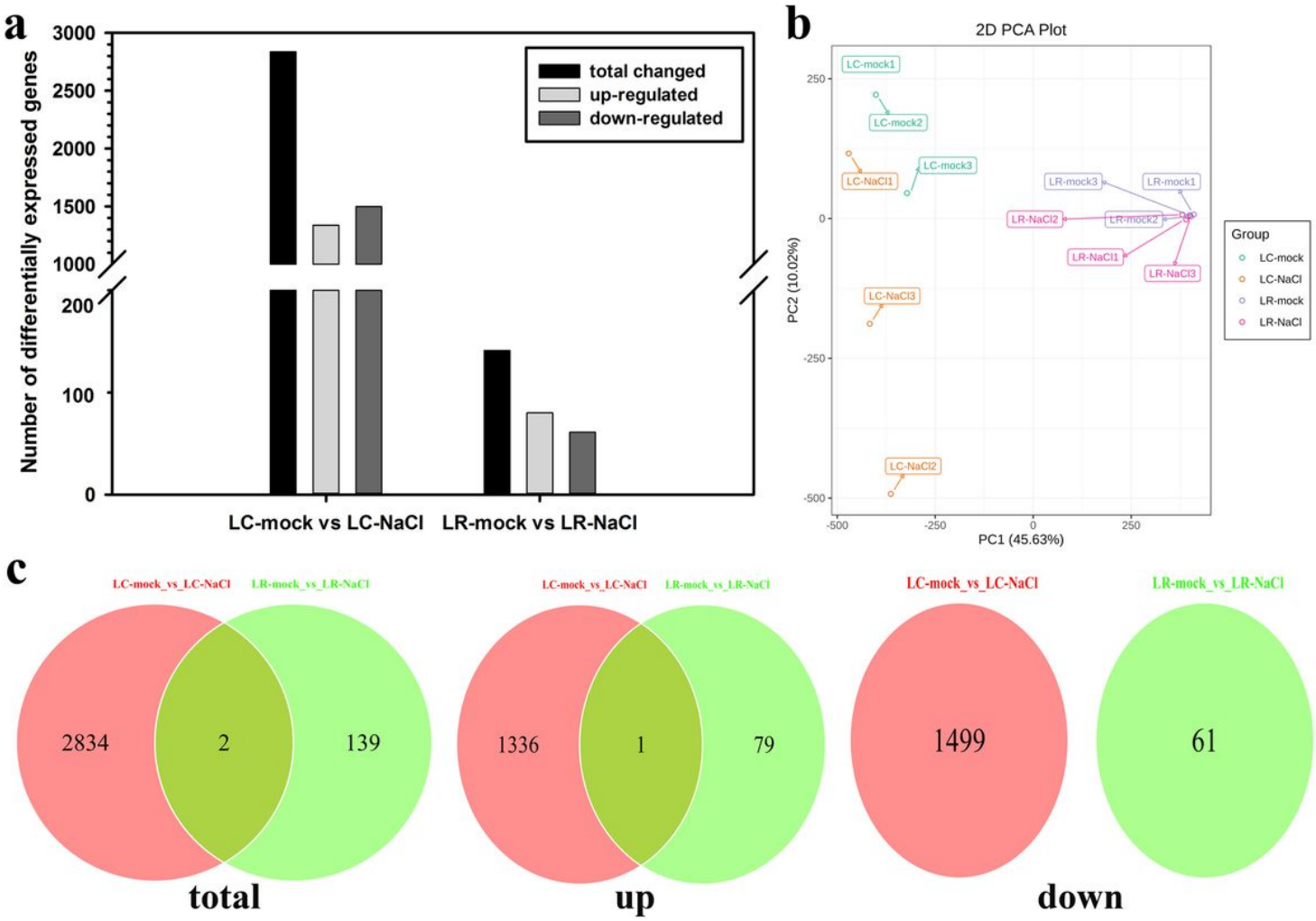

Figure 3

Transcriptome data of Lycium chinese and L. ruthenicum leaves in response to salinity stress. a Number of differentially expressed genes (DEGs) in L. chinese and L. ruthenicum under salinity stress. b PCA (Principal component analysis) clustering based on the plants' transcriptome data. c Venn diagrams of DEGs between normal and salinity stress conditions in L. chinese and L. ruthenicum.

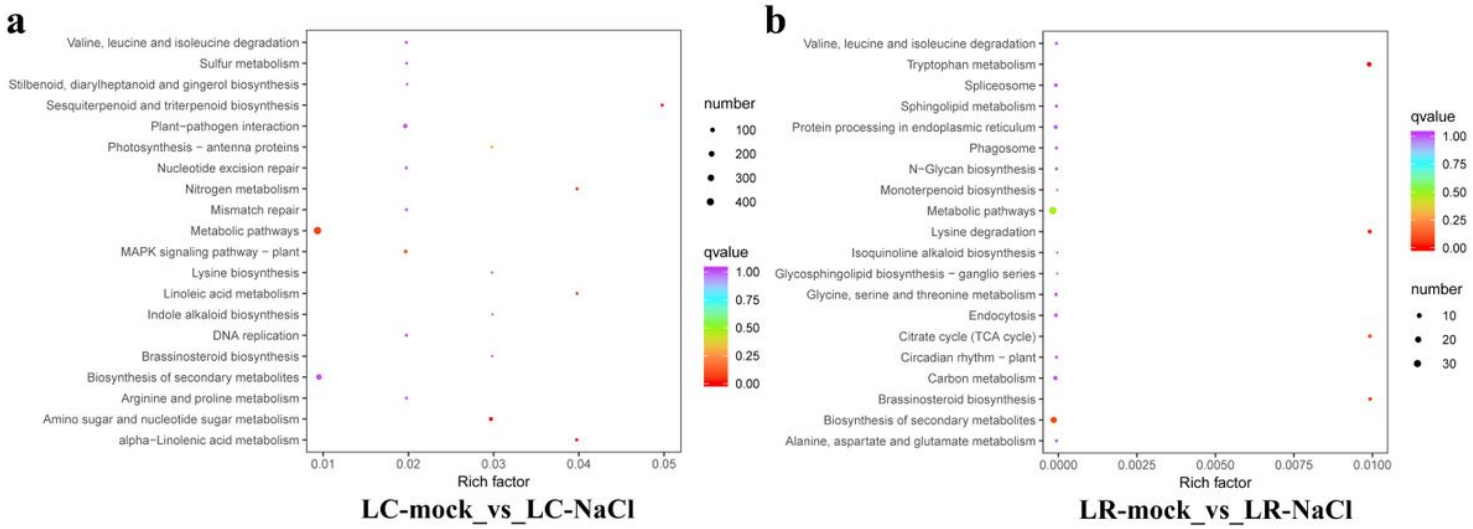

Figure 4

Statistics of KEGG enrichment analysis of DEGs (different expressed genes) in Lycium chinese (LC) and L. ruthenicum (LR) under salinity stress. a Group LC-mock vs. LC-NaCl. b Group LR-mock vs. LR-NaCl.

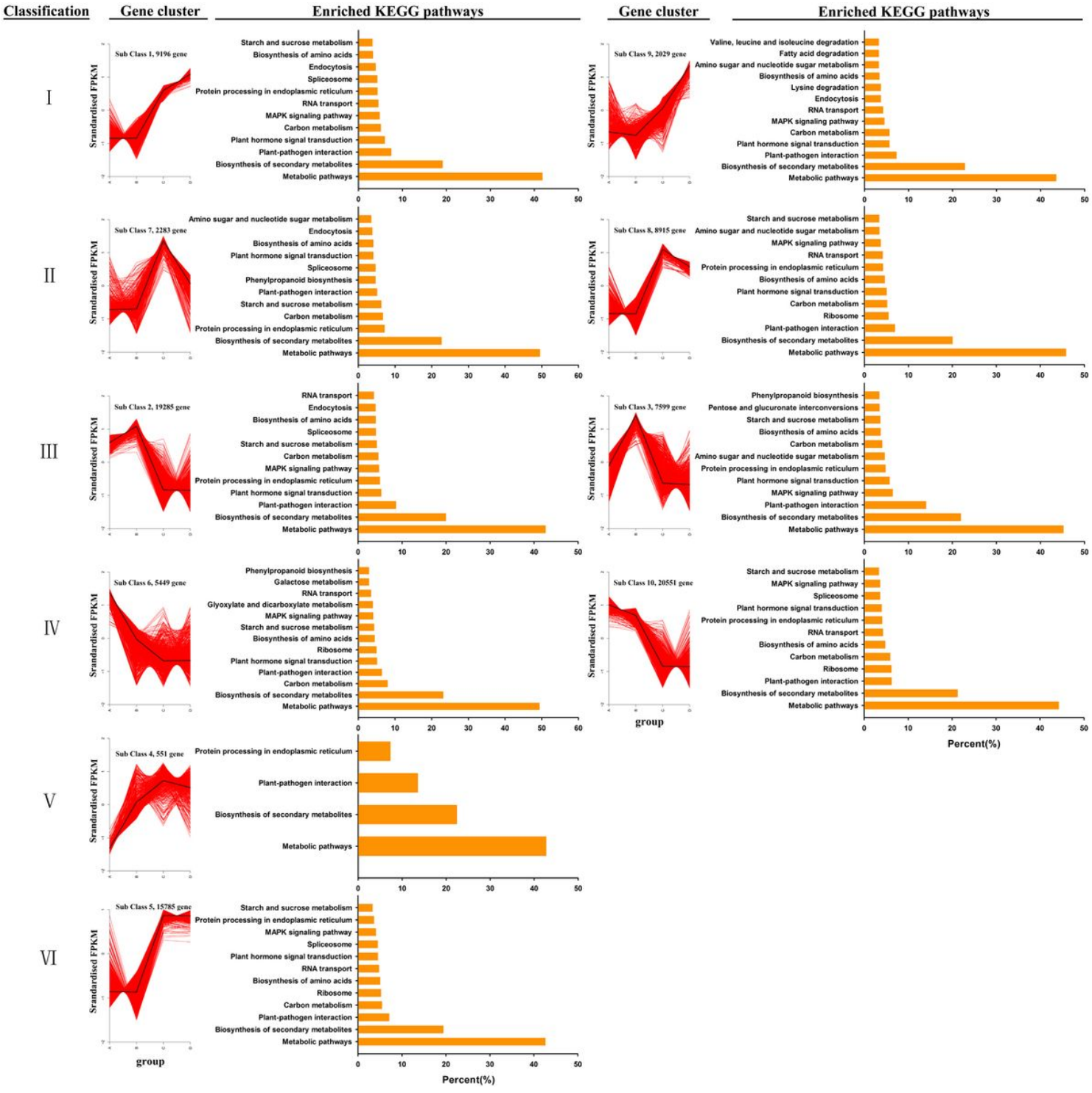

Figure 5

K-means transcriptomic analysis of significant DEGs in Lycium chinese and L. ruthenicum under control and salinity stress conditions. The DEGs are divided into 10 groups, which are classified into six types. The top 10 KEGG pathways in each group are listed on the corresponding right panel.

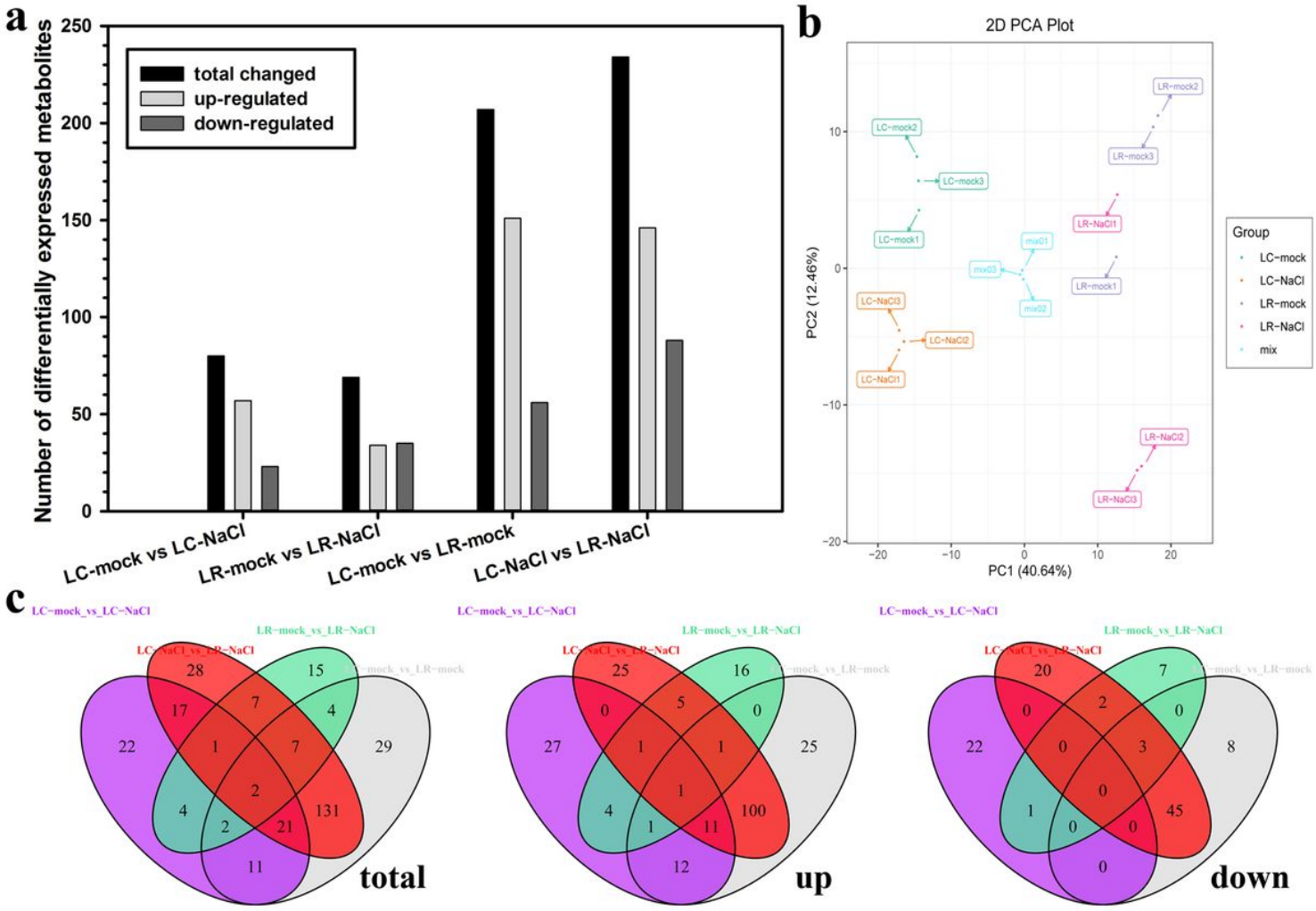

Figure 6

Metabolome analysis of Lycium chinese and L. ruthenicum in response to salinity stress. a Number of differential expressed metabolites in L. chinese and L. ruthenicum under salinity stress. b PCA (Principal component analysis) clustering based on metabolome data. c Venn diagrams of the different expressed metabolites between control and salinity stress conditions in L. chinese and L. ruthenicum.

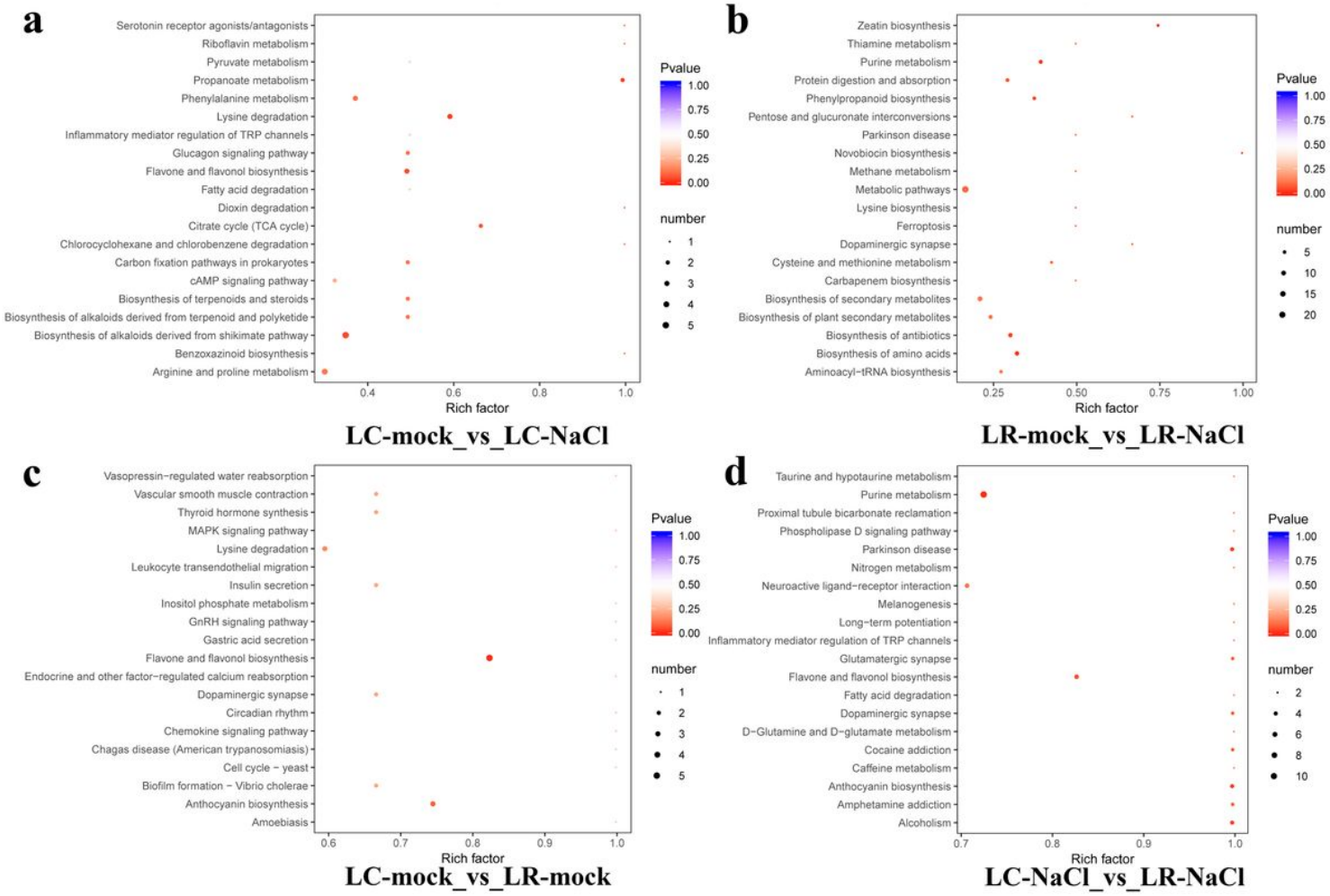

Figure 7

KEGG pathway enrichment of differential expressed metabolites in Lycium chinese (LC) and L. ruthenicum (LR) under normal and salinity stress conditions. a Group LC-mock vs. LC-NaCl. b Group LR-mock vs. LR-NaCl. c Group LC-mock vs. LR-mock. d Group LC-NaCl vs. LR-NaCl.

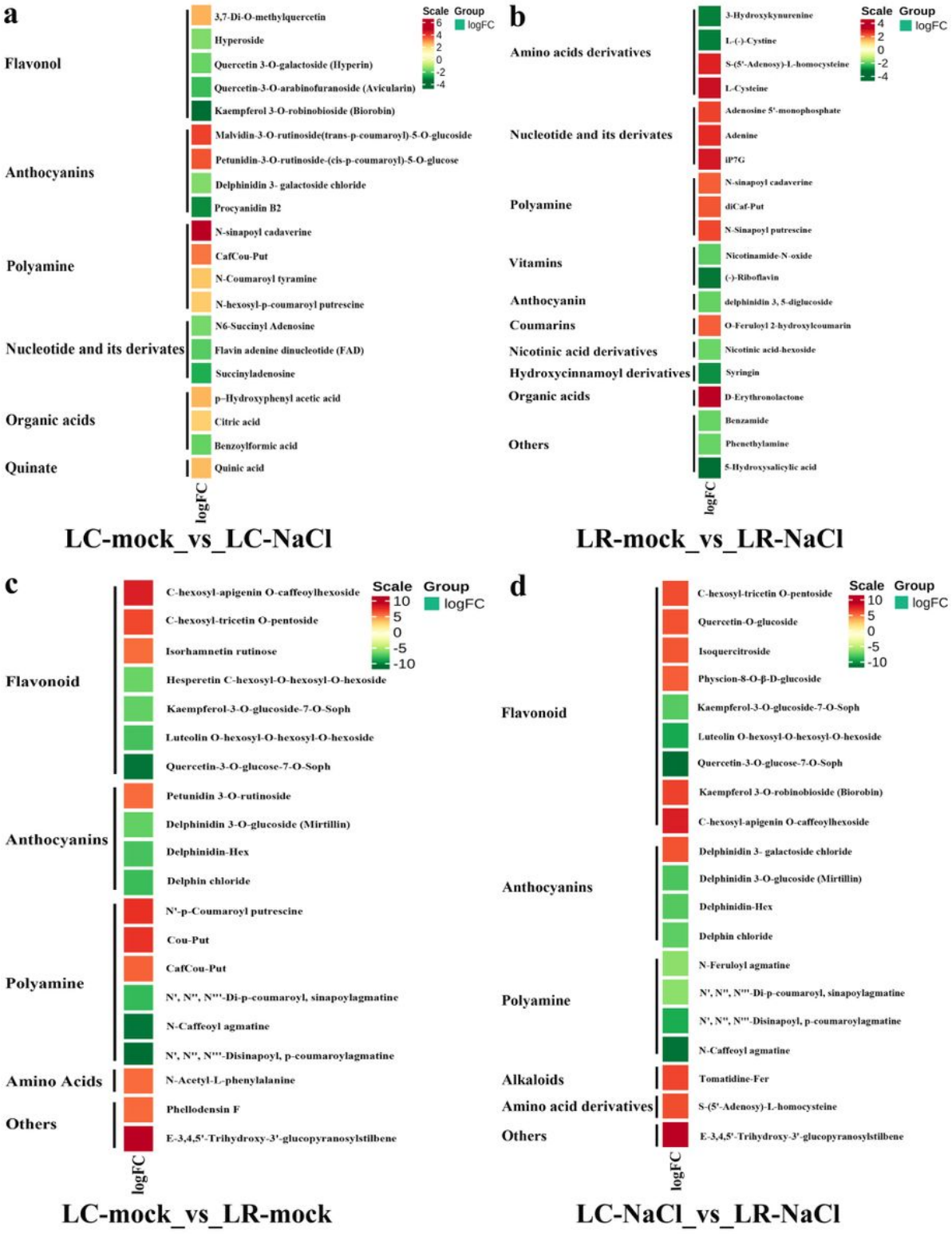

Figure 8

Heatmap of the top 20 significantly differential expressed metabolites in Lycium chinese (LC) and L. ruthenicum (LR) under control and salinity stress conditions. a Group LC-mock vs. LC-NaCl. b Group LR-mock vs. LR-NaCl. c Group LC-mock vs. LR-mock. d Group LC-NaCl vs. LR-NaCl.

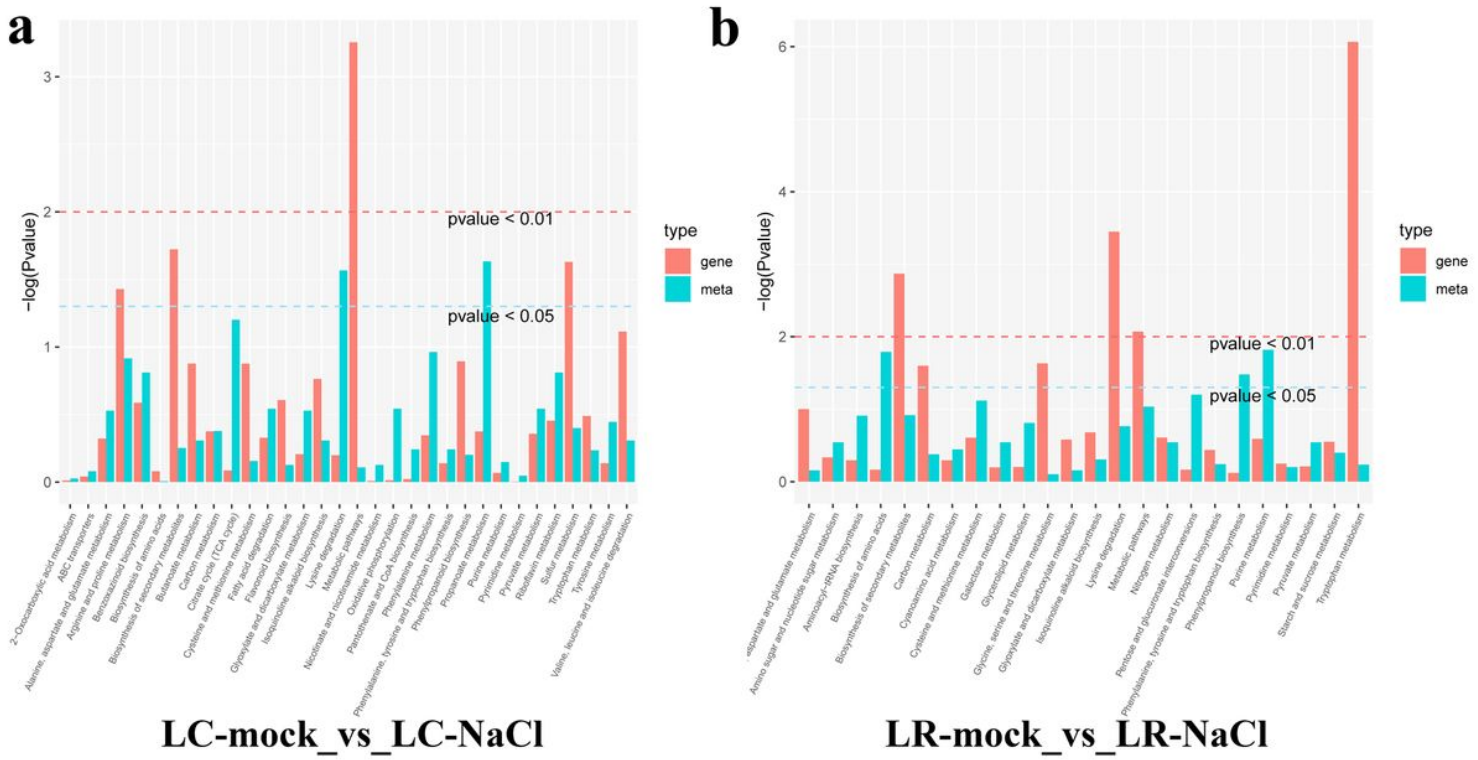

Figure 9

KEGG pathway enrichment (histogram of P-values) analysis of Lycium chinese (LC) and L. ruthenicum (LR) under normal and salinity stress conditions. a Group LC-mock vs. LC-NaCl. b Group LR-mock vs. LR-NaCl. The abscissa represents metabolic pathways, the ordinate represents enriched P-values, expressed as −log(P-value); the red and green columns respectively represents the differential expressed genes and metabolites.

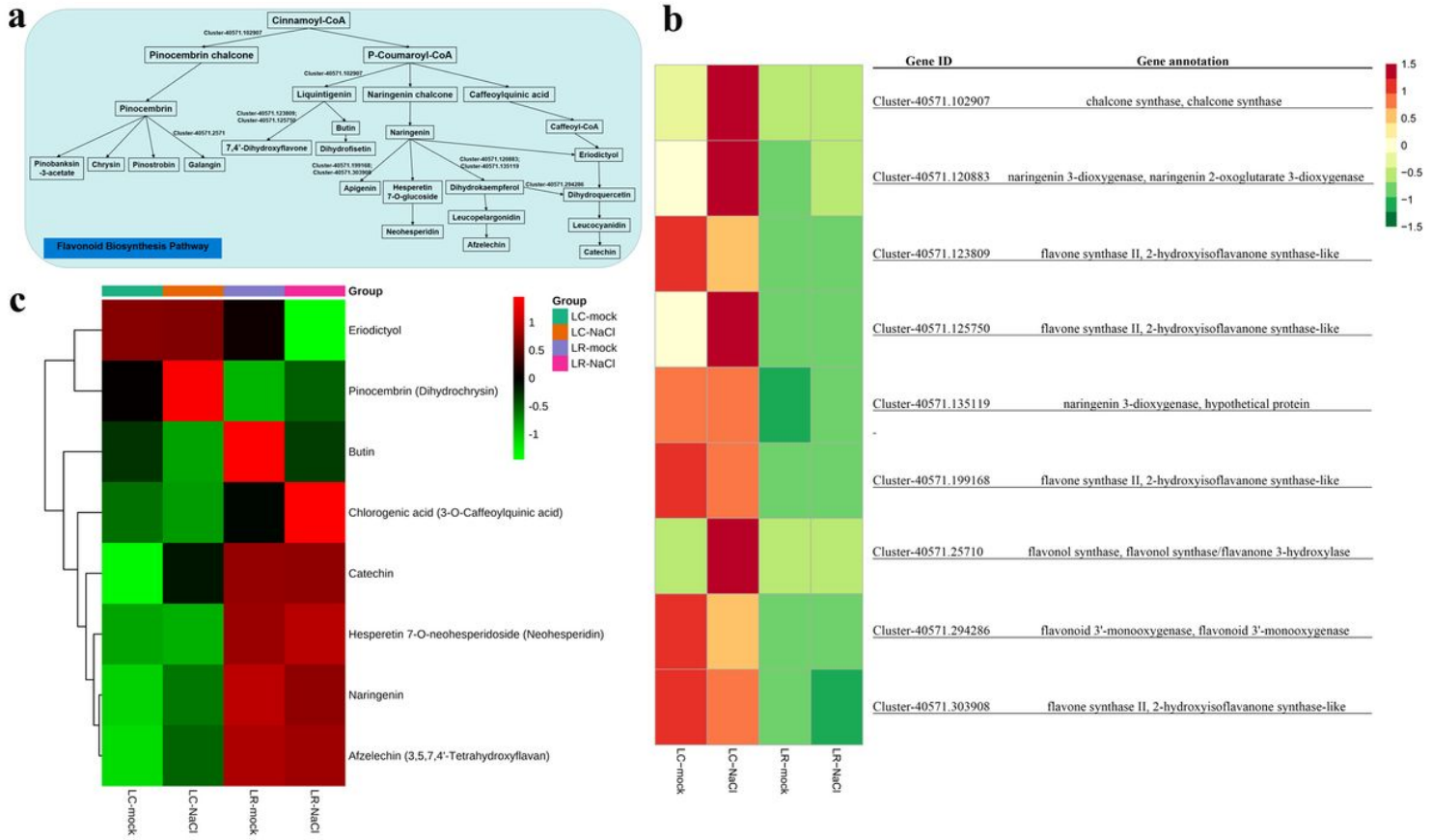

Figure 10

Adaptive changes in flavonoid metabolism in Lycium chinese and L. ruthenicum under salinity stress. a The flavonoid biosynthesis pathway. b Heatmap of DEGs (differentially expressed genes) involved in the flavonoid metabolic pathway. c Heatmap of differential expressed metabolites in the flavonoid metabolic pathway.

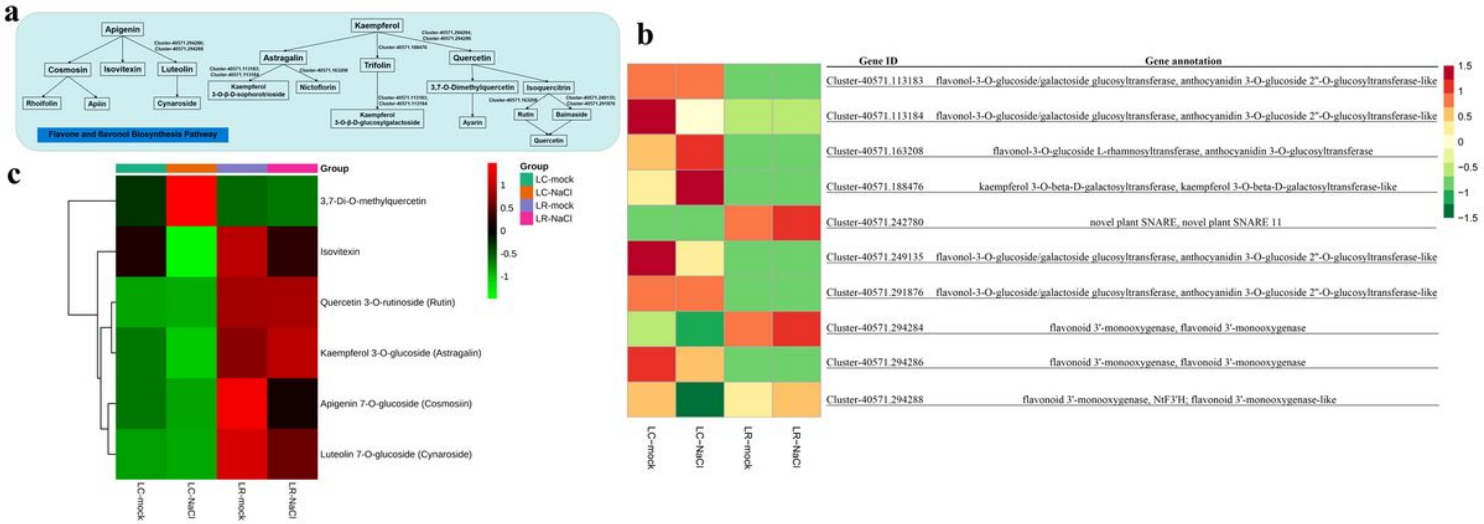

Figure 11

Alterations to flavone and flavonol metabolism in Lycium chinese and L. ruthenicum under salinity stress. a The flavone and flavonol biosynthesis pathway. b Heatmap of DEGs (differentially expressed genes) involved in the flavone and flavonol metabolic pathway. c Heatmap of differential expressed metabolites in the flavone and flavonol metabolic pathway.